Chiral topological superconductor from the quantum Hall state

Xiao-Liang Qi,[1,2] Taylor L. Hughes,[1,3] and Shou-Cheng Zhang[1]
[1]*Department of Physics, Stanford University, Stanford, California 94305, USA*
[2]*Microsoft Research, Station Q, Elings Hall, University of California, Santa Barbara, California 93106, USA*
[3]*Department of Physics, University of Illinois, 1110 West Green Street, Urbana, Illinois 61801, USA*
(Received 31 March 2010; revised manuscript received 29 September 2010; published 10 November 2010)

The chiral topological superconductor in two dimensions has a full pairing gap in the bulk and a single chiral Majorana state at the edge. The vortex of the chiral superconducting state carries a Majorana zero mode which is responsible for the non-Abelian statistics of the vortices. Despite intensive searches, this superconducting state has not yet been identified in nature. In this paper, we consider a quantum Hall or a quantum anomalous Hall state near the plateau transition and in proximity to a fully gapped *s*-wave superconductor. We show that this hybrid system may realize the chiral topological superconductor state and propose several experimental methods for its observation.

DOI: 10.1103/PhysRevB.82.184516 PACS number(s): 74.90.+n, 71.10.Pm, 03.67.Lx, 73.43.−f

I. INTRODUCTION

There are two basic types of topological states in two dimensions (2D) which break the time-reversal symmetry T. The first is the quantum Hall (QH) state which has a full gap in the bulk and gapless chiral modes at the edge. The integer number of the chiral edge modes N is a topological invariant which can be directly related to the bulk topological invariant of the QH state.[1] The quantum Hall state is realized in the presence of a large external magnetic field, however, the quantized-Hall conductance can, in principle, also be realized in topological insulators which break the T symmetry.[2,3] More recently, realistic proposals suggest that doping 2D topological insulators such as HgTe and Bi_2Te_3 with magnetic dopants,[4,5] can result in the so-called quantum anomalous Hall (QAH) insulator without an external magnetic field. The second state is the chiral superconductor which has a full pairing gap in the 2D bulk and $\mathcal{N}$ gapless chiral Majorana fermions[6,7] at the edge. The case of a chiral superconductor with $\mathcal{N}=1$ is most interesting. The edge state has half the degrees of freedom of an $N=1$ QH or QAH state, therefore, this is the minimal topological state in 2D. The vortex of such a chiral topological superconductor (TSC) carries a single Majorana zero mode,[8] giving rise to the non-Abelian statistics[9,10] which could provide a platform for topological quantum computing.[11] The simplest model for an $\mathcal{N}=1$ chiral TSC is realized in the p_x+ip_y pairing state of spinless fermions.[9] A spinful version of the chiral superconductor has been predicted to exist in Sr_2RuO_4,[12] however, the experimental situation is far from definitive. Recently, several new proposals of realizing Majorana fermion state with conventional superconductivity have been investigated by making use of strong spin-orbital coupling.[13,14]

In this paper we propose a general and intrinsic relation between QH states and the chiral TSC state, which leads to a different method to generate a chiral TSC from a QH or a QAH parent state. When a QH state is coupled to a conventional *s*-wave superconductor through the proximity effect, the topological phase transition between phases with trivial and nontrivial Hall conductance is, in general, split into two transitions, between which there is *always* a chiral TSC phase. Compared to conventional QH systems, the QAH system can realize the QH state and the topological phase transition without a large external magnetic field, which makes the proximity effect to a superconductor much easier to realize. Physically, our proposal is based on the observation that the QAH system with N chiral edge modes in proximity with a conventional superconductor is already a chiral TSC with an even number $\mathcal{N}=2N$ of chiral Majorana edge modes. Since the degeneracy among these chiral Majorana modes is lifted by the proximity to the superconductor, the transition from the QAH insulator to a topologically trivial insulator must generically pass through a chiral TSC phase with an odd number $\mathcal{N}$ of chiral Majorana edge modes. This is the interesting state with non-Abelian statistics. The proposed device is illustrated in Fig. 1.

II. QAH INSULATOR

Our proposal works both for a QH state near the plateau transition and a QAH state near the topological phase transition to a trivial insulator. For definiteness, we focus on the

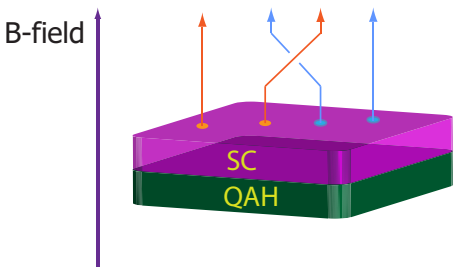

FIG. 1. (Color online) Our proposed hybrid device consists of a QAH insulator layer and a fully gapped superconductor layer on top. When the QAH insulator is close to the topological quantum phase transition, the proximity effect to the superconductor generically induces a chiral topological superconductor phase with an odd number of chiral Majorana edge modes. In the presence of a magnetic field **B**, vortices carry Majorana zero modes with non-Abelian statistics. The QAH insulator could also be replaced by a QH state near the plateau transition.

QAH case in most of our paper and comment on the generality, and the QH state near the end. We take the simplest model QAH Hamiltonian realized with low-energy states near the Γ point[3]

$$H_{\mathrm{QAH}} = \sum_{\mathbf{p}} \psi_{\mathbf{p}}^{\dagger} h_{\mathrm{QAH}}(\mathbf{p}) \psi_{\mathbf{p}},$$

$$h_{\mathrm{QAH}}(\mathbf{p}) = \begin{pmatrix} m(p) & A(p_x - ip_y) \\ A(p_x + ip_y) & -m(p) \end{pmatrix}, \tag{1}$$

where $m(p)=m+Bp^2$, A,B,m are material parameters, and $\psi_{\mathbf{p}}=(c_{p\uparrow}\ c_{p\downarrow})$. For $B=0$, this Hamiltonian is exactly the massive Dirac Hamiltonian in $2+1$ dimensions, however, the presence of the B term in the QAH Hamiltonian is crucial for determining the topological properties. In the following we will take $B>0$. The bulk energy spectrum $E_{\pm}(p) = \pm\sqrt{A^2p^2+(m+Bp^2)^2}$ is gapped as long as $m\neq 0$. The Hall conductance of any gapped system is quantized, i.e., $\sigma_H = Ne^2/h$, where N is the first Chern number in momentum space defined by[1,3]

$$N = \frac{1}{2\pi}\sum_{E_n<0}\int d^2p(\partial_x a_y^{nn} - \partial_y a_x^{nn}) \tag{2}$$

with $a_i^{nn}=-i\langle n,\mathbf{p}|\partial/\partial k_i|n,\mathbf{p}\rangle$ the Berry phase connection in momentum space and n the band index. For the specific model in Eq. (2), the Hamiltonian can be rewritten as $h_{\mathrm{QAH}} = \Sigma_a d_a(\mathbf{p})\sigma_a$ with σ_a the Pauli matrices and $d_a(\mathbf{p}) = [Ap_x, Ap_y, m(p)]$. We see that the $m(p)$ term generally breaks the T symmetry. The Chern number for Hamiltonians of this form has a simple expression[3]

$$N = \frac{1}{8\pi^2}\int d^2p\,\epsilon^{abc}\hat{d}_a\frac{\partial \hat{d}_b}{\partial p_x}\frac{\partial \hat{d}_c}{\partial p_y}, \tag{3}$$

where the unit vector $\hat{d}_a(\mathbf{p})=d_a(\mathbf{p})/\sqrt{\Sigma d_a^2(\mathbf{p})}$. According to Eq. (3), the Hall conductance is determined by the winding number of the unit vector $\hat{\mathbf{d}}(\mathbf{p})$ in momentum space. It is straightforward to see that for $m<0$ $\hat{\mathbf{d}}(\mathbf{p})$ has a Skyrmion configuration with $N=1$ while for $m>0$ the winding number is trivial $N=0$.[3] The point $m=0$ is a quantum-critical point between a trivial insulator and a QAH insulator. The QAH phase with Chern number N has N chiral edge states. In the simplest case of $N=1$, the edge state is described by the effective one-dimensional Hamiltonian $H_{\mathrm{edge}}=\Sigma_p vp\,\eta_p^{\dagger}\eta_p$, where $\eta_p^{\dagger}$ and η_p are the creation and annihilation operators of the chiral edge fermion.

III. PHASE DIAGRAM OF QAH-SC SYSTEM

In proximity to an s-wave superconductor, a finite pairing potential can be induced in the QAH state. The Bogoliubov–de Gennes (BdG) Hamiltonian for the proximity coupled QAH state is

$$H_{\mathrm{BdG}} = \frac{1}{2}\sum_{\mathbf{p}}\Psi_{\mathbf{p}}^{\dagger}\begin{pmatrix} h_{\mathrm{QAH}}(\mathbf{p})-\mu & i\Delta\sigma^y \\ -i\Delta^*\sigma^y & -h_{\mathrm{QAH}}^*(-\mathbf{p})+\mu \end{pmatrix}\Psi_{\mathbf{p}}, \tag{4}$$

where $\Psi_p=(c_{p\uparrow}\ c_{p\downarrow}\ c_{-p\uparrow}^{\dagger}\ c_{-p\downarrow}^{\dagger})^T$. Just as in the QAH case, the superconductor Hamiltonian in Eq. (4) can be classified by the Chern number $\mathcal{N}$ defined in Eq. (2) in momentum space. However, there are two key differences from the QAH case. First, for the superconductor Hamiltonian, the Chern number $\mathcal{N}$ does not physically correspond to a quantized Hall conductance because *charge* is not conserved. A superconductor with Chern number $\mathcal{N}$ has $\mathcal{N}$ edge states, similar to the QAH system, but the number of edge states is counted in the basis of chiral Majorana fermions, which are their own anti particles. For example, the edge state of an $\mathcal{N}=1$ TSC state is described by $H_{\mathrm{edge}}=\Sigma_{p\geq 0} vp\,\gamma_{-p}\gamma_p$, where the chiral Majorana fermion operators γ_p satisfy $\gamma_{-p}=\gamma_p^{\dagger}$, $\{\gamma_p,\gamma_q\}=\delta_{p+q}$. Second, a superconductor has quantized vortices. A TSC with *odd* Chern number $\mathcal{N}$ generically has a Majorana zero mode in the vortex core,[9] which is described by a Majorana operator γ_0 satisfying $[\gamma_0, H_{\mathrm{BdG}}]=0$ and $\gamma_0=\gamma_0^{\dagger}$. The Majorana zero mode is protected topologically because the energy spectrum of the BdG Hamiltonian is always symmetric around zero energy. The presence of the Majorana fermion is essential for topological quantum computing applications.[11]

We will first study the phase diagram of the system in Eq. (4) for $\mu=0$. The bulk quasiparticle spectrum is $E_{\pm}(\mathbf{p}) = \pm\sqrt{A^2p^2+[\Delta\pm m(p)]^2}$. Since topological invariants cannot change without closing the bulk gap, the phase diagram can be determined by first finding the phase boundaries which are gapless regions in the (m,Δ) plane, and then calculating the Chern number of the gapped phases. For this model the critical lines are determined by $|\Delta\pm m|=0$ which leads to the phase diagram as shown in Fig. 2(a). (Only the region $\Delta\geq 0$ is shown.) As expected, the phase boundary reduces to the critical point $m=0$ between the QAH phase and a trivial or normal insulator (NI) phase in the limit $\Delta=0$. The point $m=0$ is a multicritical point in this phase diagram. For $m>0$ and $|m|>|\Delta|$ the system is adiabatically connected to a trivial insulator state with a full gap and no edge state so it must be a trivial superconductor phase. For $m<0$ and $|m|>|\Delta|$ the system is in a nontrivial TSC state which is adiabatically connected to the QAH state in the $\Delta=0$ limit. The Chern number of this phase can be determined by the $\Delta=0$ limit, in which case the off-diagonal terms of the BdG Hamiltonian in Eq. (4) vanish. In this limit the eigenstates of H_{BdG} are determined by the eigenstates of the QAH Hamiltonian $h_{\mathrm{QAH}}(\mathbf{p})$ [Eq. (2)]. It is straightforward to check from Eq. (2) that the Chern number N_p and N_h for the particle and the hole states are both equal to that of the QAH system. In the $m<0$ phase we have $N_p=N_h=1$, leading to the total Chern number $\mathcal{N}=N_p+N_h=2$.

Similarly, the Chern number of the superconductor phase emerging at finite Δ can be determined by studying the special limit of $m=0$ [point C in Fig. 2(a)]. In this limit, Hamiltonian (4) can be block diagonalized by a basis transformation into the following form:

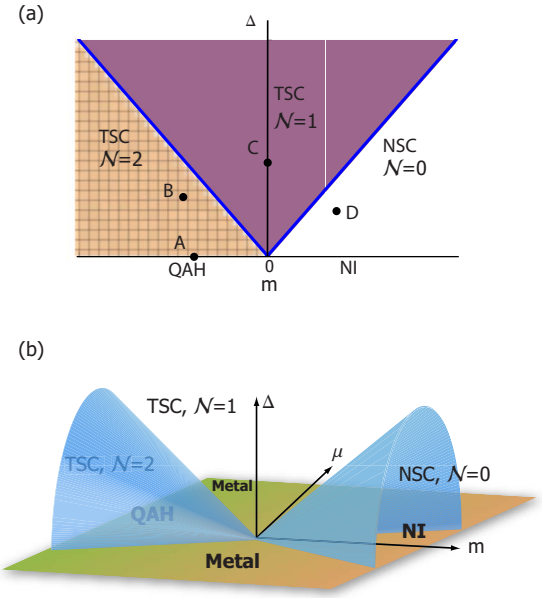

FIG. 2. (Color online) (a) Phase diagram of the QAH-SC hybrid system for $\mu=0$. The x axis labels the mass parameter m and the y axis labels the magnitude of Δ. Integers $\mathcal{N}$ label the Chern number of the superconductor, which is equal to the number of chiral Majorana edge modes. (b) Phase diagram for finite μ shown only for $\Delta \geq 0$. Phases QAH, NI, and Metal (labeled in bold) are well defined only in the $\Delta=0$ plane.

$$H_{\mathrm{BdG}}(\mathbf{p}) = \frac{1}{2}\sum_{\mathbf{p}} \tilde{\Psi}^{\dagger}_{\mathbf{p}} \begin{pmatrix} h_{+}(\mathbf{p}) & \\ & -h_{-}(-\mathbf{p})^{*} \end{pmatrix} \tilde{\Psi}_{\mathbf{p}}$$

with

$$h_{\pm}(\mathbf{p}) = \begin{pmatrix} \pm|\Delta| + Bp^2 & A(p_x - ip_y) \\ A(p_x + ip_y) & -(\pm|\Delta| + Bp^2) \end{pmatrix}. \tag{5}$$

Thus we see that the Hamiltonian is equivalent to two copies of the QAH Hamiltonian in Eq. (2) but with opposite mass parameters $m=\pm|\Delta|$. The Chern number of $h_{+}(\mathbf{p})$ is trivial and that of $h_{-}(\mathbf{p})$ is $N=1$ so that the total Chern number of this TSC state is $\mathcal{N}=1$. In other words, we have proven that a TSC phase with odd Chern number $\mathcal{N}=1$ emerges in the neighborhood of the quantum-critical point between the QAH insulator and trivial insulator phases.

Next, we consider $\mu \neq 0$ in the Hamiltonian in Eq. (4), which corresponds to proximity induced superconductivity in a *doped* QAH system. Practically, the proximity effect is expected to be stronger in this case due to the finite density of states at the Fermi level. Similar to the $\mu=0$ case, we determine the phase boundaries by the gapless regions in the energy spectrum, which leads to the following condition:

$$\Delta^2 + \mu^2 = m^2.$$

The entire phase diagram in the (m, μ, Δ) space is shown in Fig. 2(b). Except for the metallic phase in the $\Delta=0$ plane with $|\mu|>m$, and the phase boundaries, there are three-gapped phases. The Chern number of each phase can be determined by its adiabatic connection to the $\mu=0$ limit. It can be seen from the phase diagram that a wide TSC phase with Chern number $\mathcal{N}=1$ emerges between the $\mathcal{N}=2$ and $\mathcal{N}=0$ phases, which are adiabatically connected to the QAH and trivial insulator phases, respectively.

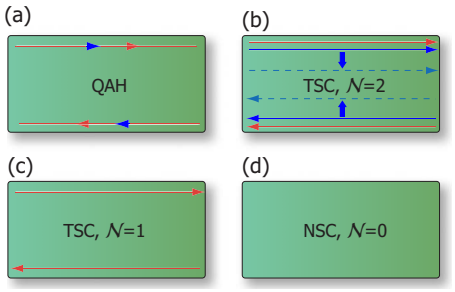

FIG. 3. (Color online) Evolution of the edge states. The four panels (a), (b), (c), and (d) correspond to the edge state configuration of points A, B, C, and D in Fig. 2(a), respectively. (a) and (b) show that a single chiral edge mode of the QAH state can be decomposed into two chiral Majorana edge modes of the TSC state. Proximity coupling to the SC state lifts the degeneracy and one pair of the chiral Majorana states can be annihilated in the bulk, giving rise to a chiral TSC state with a single chiral Majorana edge mode as shown in (c). Further changes in the parameters can cause a phase transition into the trivial or normal SC state as shown in (d).

IV. EDGE PICTURE

An intuitive way to understand such a TSC phase emerging near the QAH/NI transition is through the evolution of the edge states. As was discussed earlier, the edge state of the QAH state [e.g., the point A in the phase diagram in Fig. 2(a)] is described by the effective one-dimensional Hamiltonian $H_{\mathrm{edge}}=\Sigma_p v p \eta^{\dagger}_p \eta_p$. We can decompose the complex fermion operator into its real parts, $\eta_{p_y}=1/\sqrt{2}(\gamma_{p_y 1}+i\gamma_{p_y 2})$ and $\eta^{\dagger}_{p_y}=1/\sqrt{2}(\gamma_{-p_y 1}-i\gamma_{-p_y 2})$, where $\gamma_{p_y a}$ are Majorana fermion operators satisfying $\gamma^{\dagger}_{p_y a}=\gamma_{-p_y a}$ and $\{\gamma_{-p_y a}, \gamma_{p'_y b}\} = \delta_{ab}\delta_{p_y p'_y}$. The Hamiltonian now becomes

$$H_{\mathrm{edge}} = \sum_{p_y \geq 0} p_y(\gamma_{-p_y 1}\gamma_{p_y 1} + \gamma_{-p_y 2}\gamma_{p_y 2}) \tag{6}$$

up to a trivial shift of the energy. In comparison with the edge theory of the chiral TSC state, we see that the QAH edge state can be considered as two identical copies of chiral Majorana fermions so that the QAH phase with Chern number $N=1$ can be considered as a TSC state with Chern number $\mathcal{N}=2$, *even for infinitesimal pairing amplitudes*. This is consistent with the Chern number analysis of the bulk Hamiltonian discussed earlier.

When $\Delta \neq 0$, the constraint between the two chiral Majorana modes $\gamma_{p_y 1}$ and $\gamma_{p y 2}$ is lifted and they evolve independently. An easy way to see this is to consider the width of the edge states along the direction perpendicular to the edge. At $\Delta=0$, the edge state at $k=0$ has a width[15] $\xi \sim A/|m|$. For finite pairing their width can be estimated by $\xi_1 \sim A/|m-\Delta|$, $\xi_2 \sim A/|m+\Delta|$. As Δ increases, the localization length of one of the edge modes begins to diverge and the corresponding Majorana modes gradually move into the bulk, as shown schematically in Fig. 3(b). At the critical

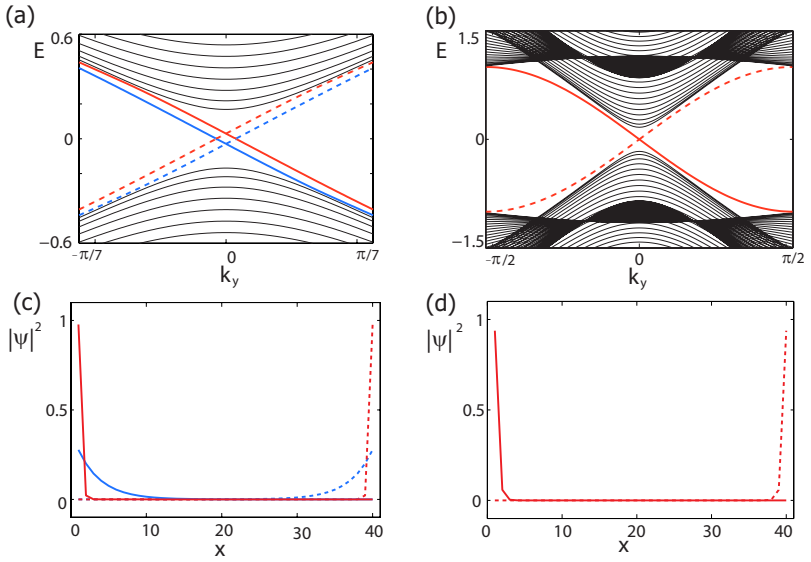

FIG. 4. (Color online) Energy spectrum of H_{BdG} versus k_y in a cylinder geometry with periodic boundary conditions in the y direction. The calculation is done for $m=-0.5$, $A=B=1.0$ with a regularization lattice constant $a=1$ and length $L_x=40$ along the x direction (see text). The system has two edge states on each edge for $\Delta=0.35$ as shown in (a) and one edge state on each edge for $\Delta=0.75$ as shown in (b). The edge states on the left (right) edge are labeled by solid (dashed) lines. In (a) the two edge states on the same edge are artificially split as a guide for the eye. (c) and (d) show the real-space probability distribution of the edge states corresponding to (a) and (b), respectively. The steeper (red) and smoother (blue) curves in (c) correspond to the edge states shifted slightly up (red) and down (blue) in (a), respectively.

pairing strength $|\Delta|=|m|$ this edge state has completely merged into the bulk states and the system is gapless. For $|\Delta|>|m|$ a gap opens again in the bulk and we are left with a single chiral Majorana edge mode. When the mass is increased toward the trivial direction, such as from points C to D in Fig. 2(a), the width of the remaining edge state increases and finally merges into the bulk at the critical line, leaving a trivial-gapped superconductor on the other side of the transition.

To directly verify this edge state evolution picture, we have also studied the edge states numerically on a cylinder geometry with periodic boundary conditions in the y direction and open boundary conditions in the x direction. The BdG Hamiltonian in Eq. (4) can be regularized on a square lattice by the simple substitution $p_{x,y}\rightarrow a^{-1}\sin(p_{x,y}a)$, $p^2=2-2a^{-2}(\cos p_x a+\cos p_y a)$ with a the lattice constant used in the discretization. For $a\rightarrow 0$ the lattice model has the same properties as the continuum model. The energy dispersion and edge state probability density for the points B and C in the phase diagram Fig. 2(a) are shown in Fig. 4. As expected, two chiral edge states with different penetration lengths exist on each edge for the $\mathcal{N}=2$ phase and only one chiral edge state exists for the $\mathcal{N}=1$ phase. Thus we see that the edge state of the QAH can be considered as two copies of chiral Majorana fermions. The topological phase transitions are given by the annihilation of these two Majorana fermions, which has to occur simultaneously if charge is conserved ($\Delta=0$) but can generically occur at two separate transitions at finite pairing strength. Consequently, the system must be in a TSC phase with odd Chern number between the two transitions.

V. DISCUSSION AND EXPERIMENTAL REALIZATION

In summary, we have shown that the proximity of a QH or a QAH system with an s-wave superconductor provides a different realization of a chiral TSC, the vortex of which has non-Abelian statistics. Although the simple model in Eq. (2) of the $N=1$ QAH state has been used to give an explicit example, it is straightforward to see that this approach toward TSC is generic and applies to any QH or QAH system near a topological phase transition. In general, a QH or a QAH state with Hall conductance Ne^2/h becomes a TSC with Chern number $\mathcal{N}=2N$ when an *infinitesimal* pairing strength is introduced by the proximity effect. Consequently, two neighboring quantum Hall phases with Hall conductance Ne^2/h and $(N-1)e^2/h$ become TSC phases with Chern number $\mathcal{N}=2N$ and $\mathcal{N}=2N-2$, between which a TSC phase with Chern number $\mathcal{N}=2N-1$ generally emerges. Our proposal is different from that of Ref. 13 since the latter preserves time-reversal symmetry and is not a purely two-dimensional state while the state studied here is a realization of the two-dimensional chiral superconductor. Our proposal is independent of the details of the superconductor which provides the proximity effect, as long as the proximity-induced superconducting gap is a full gap with no node. Our conclusion also applies to an ordinary quantum Hall system near a plateau transition, provided the magnetic field responsible for the QH state is less than the upper critical field of the superconductor. For example, InAs quantum wells and graphene are possible candidate materials. The advantage of QAH system is the absence of large magnetic field, which makes the superconducting proximity effect much easier.

There are two realistic proposals of QAH states, Mn-doped HgTe quantum wells[4] and Cr- or Fe-doped Bi_2Se_3 thin films.[5] The latter is proposed to be ferromagnetic, which thus can have quantized-Hall conductance at zero magnetic field. The former is known to be paramagnetic for small Mn concentration but only a small magnetic field is needed to polarize the Mn spin and drive the system into the QAH phase.

This is not so prohibitive because a magnetic field is necessary to generate superconducting vortices and the associated Majorana zero modes anyway. Once such a heterostructure of a QAH insulator and superconductor is fabricated, the existence of a Majorana fermion zero mode in the vortex core can be verified by scanning tunneling microscopy measurements of the local density of states in the vortex core. Several existing proposals of detecting the Majorana nature of the edge state and vortex core zero mode such as by Josephson effect,[16–18] charge transport,[19,20] or nonlocal tunneling,[21] may also apply to our system, although they are proposed in different physical systems.

ACKNOWLEDGMENTS

This work is supported by the NSF under Grant No. DMR-0904264. X.L.Q acknowledges the support of Microsoft Research Station Q. T.L.H. was supported in part by NSF under Grant No. DMR-0758462 and by the ICMT.

[1] D. J. Thouless, M. Kohmoto, M. P. Nightingale, and M. den Nijs, Phys. Rev. Lett. **49**, 405 (1982).
[2] F. D. M. Haldane, Phys. Rev. Lett. **61**, 2015 (1988).
[3] X. L. Qi, Y. S. Wu, and S. C. Zhang, Phys. Rev. B **74**, 085308 (2006).
[4] C.-X. Liu, X.-L. Qi, X. Dai, Z. Fang, and S.-C. Zhang, Phys. Rev. Lett. **101**, 146802 (2008).
[5] R. Yu, W. Zhang, H. Zhang, S. Zhang, X. Dai, and Z. Fang, Science **329**, 61 (2010).
[6] R. Jackiw and P. Rossi, Nucl. Phys. B **190**, 681 (1981).
[7] F. Wilczek, Nat. Phys. **5**, 614 (2009).
[8] G. E. Volovik, Pis'ma Zh. Eksp. Teor. Fiz. **70**, 601 (1999) [JETP Lett. **70**, 609 (1999)].
[9] N. Read and D. Green, Phys. Rev. B **61**, 10267 (2000).
[10] D. A. Ivanov, Phys. Rev. Lett. **86**, 268 (2001).
[11] C. Nayak, S. H. Simon, A. Stern, M. Freedman, and S. D. Sarma, Rev. Mod. Phys. **80**, 1083 (2008).
[12] A. P. Mackenzie and Y. Maeno, Rev. Mod. Phys. **75**, 657 (2003).
[13] L. Fu and C. L. Kane, Phys. Rev. Lett. **100**, 096407 (2008).
[14] J. D. Sau, R. M. Lutchyn, S. Tewari, and S. Das Sarma, Phys. Rev. Lett. **104**, 040502 (2010).
[15] M. König, H. Buhmann, L. W. Molenkamp, T. Hughes, C.-X. Liu, X.-L. Qi, and S.-C. Zhang, J. Phys. Soc. Jpn. **77**, 031007 (2008).
[16] L. Fu and C. L. Kane, Phys. Rev. B **79**, 161408 (2009).
[17] R. Lutchyn, J. Sau, and S. Das Sarma, Phys. Rev. Lett. **105**, 077001 (2010).
[18] Y. Tanaka, T. Yokoyama, and N. Nagaosa, Phys. Rev. Lett. **103**, 107002 (2009).
[19] A. R. Akhmerov, J. Nilsson, and C. W. J. Beenakker, Phys. Rev. Lett. **102**, 216404 (2009).
[20] L. Fu and C. L. Kane, Phys. Rev. Lett. **102**, 216403 (2009).
[21] L. Fu, Phys. Rev. Lett. **104**, 056402 (2010).